

On homotopy continuation based singularity distance computations for 3-RPR manipulators

Aditya Kapilavai and Georg Nawratil

Institute of Discrete Mathematics and Geometry, TU Wien, Austria
e-mail: {akapilavai, nawratil}@geometrie.tuwien.ac.at

Abstract. It is known that parallel manipulators suffer from singular configurations. Evaluating the distance between a given configuration to the closest singular one is of interest for industrial applications (e.g. singularity-free path planning). For parallel manipulators of Stewart-Gough type, geometric meaningful distance measures are known, which are used for the computation of the singularity distance as the global minimizer of an optimization problem. In the case of hexapods and linear pentapods the critical points of the corresponding polynomial Lagrange function cannot be found by the Gröbner basis method due to the degree and number of unknowns. But this polynomial system of equations can be solved by software tools of numerical algebraic geometry relying on homotopy continuation. To gain experiences for the treatment of the mentioned spatial manipulators, this paper attempts to find minimal multi-homogeneous Bézout numbers for the homotopy continuation based singularity distance computation with respect to various algebraic motion representations of planar Euclidean/equiform kinematics. The homogenous and non-homogenous representations under study are compared and discussed based on the 3-RPR manipulator.

Key words: 3-RPR manipulator, singularity distance, homotopy continuation, Bézout number

1 Introduction

A 3-RPR manipulator (cf. Fig. 1) is a three degree-of-freedom (dof) planar parallel manipulator (two translational and one rotational dof) where each leg is composed of a revolute joint (R)¹, a prismatic joint (P) and a further R-joint. The manipulator is actuated by changing the three lengths of the prismatic joints.

According to [10], the distance between two poses of the moving platform can be computed as:

$$d_3 := \sqrt{\frac{1}{3} \sum_{i=1}^3 \langle \mathbf{P}_i^\alpha - \mathbf{P}_i^\gamma, \mathbf{P}_i^\alpha - \mathbf{P}_i^\gamma \rangle} \quad (1)$$

where $\mathbf{P}_i^\gamma = (x_i^\gamma, y_i^\gamma)^T$ (resp. $\mathbf{P}_i^\alpha = (x_i^\alpha, y_i^\alpha)^T$) denotes the i th platform anchor point in the given (resp. α -transformed) manipulator configuration for $i = 1, 2, 3$. Both

¹ We consider R-joints as points and refer them as base/platform anchor points.

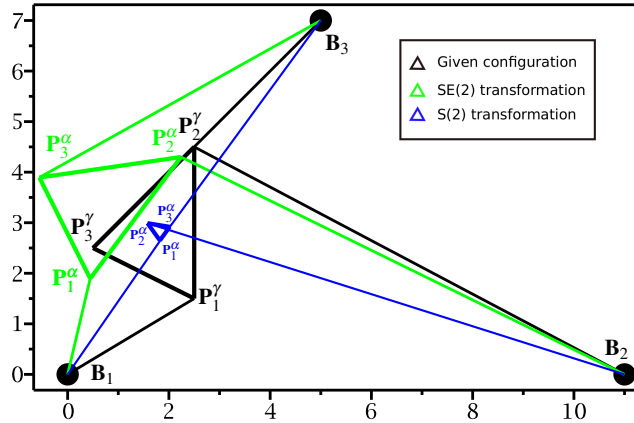


Fig. 1 3-RPR manipulator: The results obtained in this paper are based on the illustrated example taken from [10, Section 3] for $\phi = \frac{\pi}{2}$. The given configuration is illustrated in black and the closest singular one under Euclidean/equiform transformations of the platform is displayed in green/blue.

coordinate vectors \mathbf{P}_i^γ and \mathbf{P}_i^α are computed with respect to the fixed frame and $\langle \cdot, \cdot \rangle$ denotes the standard scalar product. The coordinate vectors of the platform anchor points with respect to the moving frame are given by $\mathbf{P}_i = (x_i, y_i)^T$. Moreover it was mentioned in [10] that α has not to be restricted to the planar Euclidean motion group $SE(2)$, but it can also be an element of the planar equiform motion group $S(2)$ or an affine motion.

It is well known that the α -transformed configuration is singular if and only if the carrier lines of three legs intersect in a common point or are parallel. This line-geometric characterization is equivalent to the algebraic condition $V_3 = 0$ with

$$V_3 = \det \begin{pmatrix} \mathbf{P}_1^\alpha - \mathbf{B}_1 & \mathbf{P}_2^\alpha - \mathbf{B}_2 & \mathbf{P}_3^\alpha - \mathbf{B}_3 \\ \det(\mathbf{B}_1, \mathbf{P}_1^\alpha - \mathbf{B}_1) & \det(\mathbf{B}_2, \mathbf{P}_2^\alpha - \mathbf{B}_2) & \det(\mathbf{B}_3, \mathbf{P}_3^\alpha - \mathbf{B}_3) \end{pmatrix} \quad (2)$$

where \mathbf{B}_i denotes the coordinate vector of the i th base anchor point with respect to the fixed system. For determining the singularity distance one has to find the transformation α that minimizes Eq. (1) under the side condition that $V_3 = 0$ holds. For $\alpha \in SE(2)$ we denote the singularity distance by s_3 and for $\alpha \in S(2)$ by e_3 , respectively. For the determination of s_3 and e_3 we compute the critical points of the corresponding polynomial Lagrange function L , i.e. the zero set of the polynomial system of equations arising from the partial derivatives of L . Finally, one only has to pick out the solution which yields the global minimum.

Commonly, Newton's method is simple and quick to solve a polynomial system. However, in general it only converges when a good initial guess is used, and even then this only yields one solution. In contrast, the homotopy continuation method allows an efficient and reliable computation of all solutions to polynomial systems. The newest open-source numerical continuation software packages are Homotopy-

Continuation.jl [3] and Bertini 1.6v [1]. These packages and other available software and their performances are compared in [3]. We have chosen Bertini 1.6v for computing the singularity distance of parallel manipulators due to (a) its exceptional features mentioned in [12, p. 156] which will be useful for our future research and (b) the longevity of the Bertini software.

Under the default settings, declaration of all unknown variables n of the polynomial system into a single *variable group* causes Bertini to form a *total-degree homotopy*, which in general does not result in a minimal Bézout number. The partition of the variables into multiple groups lead to a *multi-homogeneous homotopy*. The grouping of the n unknown variables affects the resulting minimal multi-homogeneous Bézout number² (B_{min}). As Bertini does not group the variables automatically, the user is responsible for choosing the variable groups in a way that a minimal multi-homogeneous Bézout number (B_{min}) is obtained, which improves the computational costs/time. For this purpose, attempts have been made on search algorithms (e.g. [11, 6]) to find the optimal partition of variables groups, but in [2, p. 72] it is stated that “*there does not yet exist a truly efficient algorithm for finding optimal groupings, and the combinatorics are such that an exhaustive examination of all possible groupings becomes impractical as the number of variables grows much larger than 10*”. Investigating the optimal variable group search algorithms is out of the scope of the paper, but as mentioned in [2, p. 73], “*with a little practice, a user can identify and check the most promising candidates*” resulting in B_{min} .

According to [2, p. 96] the “*use of isotropic coordinates is advantageous when applying multi-homogeneous homotopy, since it converts many of the quadratic expressions that appear in planar kinematics into bilinear expressions*” but no attempts have been made so far to compare this approach with other algebraic motion representations. Hence, we determine B_{min} for the singularity distance computation of 3-RPR manipulators based on homotopy continuation with respect to various algebraic motion representations of SE(2) and S(2). In addition this study is useful to gain experience for the spatial case.

The rest of the paper is organized as follows: We divide the investigated algebraic motion representations into two classes, namely the non-homogenous ones (Sec. 2) and the homogenous ones (Sec. 3). In both of these two sections we give a brief introduction of the representations followed by the discussion of the results. Finally, Section 4 concludes the paper.

2 Non-Homogeneous Representations

In this section, we present three non-homogeneous algebraic representations for each of the motion groups SE(2) and S(2), respectively.

² The Bézout number of a system of multi-homogeneous polynomial equations is the largest number of non-singular solutions such a system can have, and it is also the number of solution paths used to compute all geometrically isolated solutions of the system using multi-homogeneous polynomial continuation [11].

Point Based Representation (PBR): We call the approach given in [10] *point based representation* as the transformation is formulated in terms of the first and second platform anchor points. For the third platform point the transformation reads as

$$\mathbf{P}_3^\alpha = \frac{1}{\sqrt{(x_2-x_1)^2+(y_2-y_1)^2}} \begin{pmatrix} x_2^\alpha - x_1^\alpha & y_1^\alpha - y_2^\alpha \\ y_2^\alpha - y_1^\alpha & x_2^\alpha - x_1^\alpha \end{pmatrix} \begin{pmatrix} x_3 - x_1 \\ y_3 - y_1 \end{pmatrix} + \mathbf{P}_1^\alpha. \quad (3)$$

Then the Lagrange function L for the computation of e_3 can be written as

$$L: d_3^2 - \lambda V_3 = 0. \quad (4)$$

The additional constraint $M = 0$ with $M := \overline{\mathbf{P}_1^\alpha \mathbf{P}_2^\alpha}^2 - \overline{\mathbf{P}_1 \mathbf{P}_2}^2$ results in the computation of s_3 from the Lagrange function

$$L: d_3^2 - \lambda V_3 - \mu M = 0. \quad (5)$$

Planar Euler-Rodrigues Representation (PERR): Using this representation the transformation $\alpha: \mathbb{R}^2 \rightarrow \mathbb{R}^2$ can be written as

$$\alpha: \mathbf{P}_i \mapsto \mathbf{P}_i^\alpha := \begin{pmatrix} a_1^2 - a_2^2 & -2a_1a_2 \\ 2a_1a_2 & a_1^2 - a_2^2 \end{pmatrix} \mathbf{P}_i + \begin{pmatrix} a_3 \\ a_4 \end{pmatrix} \quad \text{with } a_1, \dots, a_4 \in \mathbb{R}. \quad (6)$$

The computation of e_3 and s_3 is based on the same Lagrange function as for the PBR with the sole difference that M is given by $M := a_1^2 + a_2^2 - 1$.

Isotropic Coordinates Representation (ICR): Using this approach the point \mathbf{P}_i is represented by the pair (z_i, \bar{z}_i) of conjugate complex numbers with $z_i = x_i + iy_i$. This isotropic coordinates are transformed by $\alpha: \mathbb{C}^2 \rightarrow \mathbb{C}^2$ as follows (e.g. [9]):

$$\alpha: (z_i, \bar{z}_i) \mapsto (z_i^\alpha, \bar{z}_i^\alpha) := (\kappa z_i + \tau, \tilde{\kappa} \bar{z}_i + \tilde{\tau}) \quad \text{with } \kappa, \tau, \tilde{\kappa}, \tilde{\tau} \in \mathbb{C}. \quad (7)$$

Note that $(z_i^\alpha, \bar{z}_i^\alpha)$ is a real point if and only if $\bar{z}_i^\alpha = \overline{z_i^\alpha}$ holds; i.e. $\tilde{\kappa} = \overline{\kappa}$ and $\tilde{\tau} = \overline{\tau}$. Again the computation of e_3 and s_3 is based on the same Lagrange function as for the PBR with the sole difference that M is given by $M := \kappa \tilde{\kappa} - 1$.

In summary the transformation α is given by the non-homogenous 4-tuple $(x_1^\alpha, y_1^\alpha, x_2^\alpha, y_2^\alpha)$ in PBR, (a_1, a_2, a_3, a_4) in PERR and $(\kappa, \tau, \tilde{\kappa}, \tilde{\tau})$ in ICR, respectively.

Table 1 Comparison of Bézout numbers for all studied representations of SE(2)

Method	Best groupings	B_{min}	T_{avg}	Worst groupings	B_{max}	DOL
PBR	$\{(x_1^\alpha, y_1^\alpha, x_2^\alpha, y_2^\alpha), (\lambda, \mu)\}$	144	1 800	$\{(x_1^\alpha), (x_2^\alpha, \mu), (y_1^\alpha, \lambda), (y_2^\alpha)\}$	8 448	4
PERR	$\{(a_1, a_2), (a_3, a_4), (\lambda, \mu)\}$	360	45 920	$\{(x_1^\alpha, \mu), (y_2^\alpha, \lambda), (x_2^\alpha), (y_1^\alpha)\}$	8 448	6
ICR	$\{(\kappa), (\tilde{\kappa}), (\lambda), (\mu), (\tau, \tilde{\tau})\}$	360	35 640	$\{(a_1, \lambda, a_3), (a_2, \mu, a_4)\}$	50 992	4
		136	249 880	$\{(a_1, \mu, a_4), (a_2, \lambda, a_3)\}$	50 992	
				$\{(\kappa, \tilde{\tau}), (\tilde{\kappa}, \mu, \tau, \lambda)\}$	2 187	
				$\{(\kappa, \mu, \lambda, \tilde{\tau}), (\tilde{\kappa}, \tau)\}$	2 187	
BGR	$\{(e_0, e_3, t_1, t_2)_h, (\lambda)\}$	300	122 180	–	–	5
DCKR	$\{(\theta, \tilde{\theta}, \sigma, \tilde{\sigma})_h, (\lambda)\}$	300	115 283	–	–	4

Table 2 Comparison of Bézout numbers for all studied representations of S(2)

Method	Best groupings	B_{min}	T_{avg}	Worst groupings	B_{max}	DOL
PBR	$\{(x_1^\alpha, y_1^\alpha, x_2^\alpha, y_2^\alpha), (\lambda)\}$	96	970	$\{(x_1^\alpha, y_1^\alpha), (x_2^\alpha, y_2^\alpha), (\lambda)\}$	1 296	4
PERR	$\{(a_1, a_2), (a_3, a_4), (\lambda)\}$	828	73 000	$\{(x_1^\alpha, y_2^\alpha), (y_1^\alpha, x_2^\alpha), (\lambda)\}$ $\{(a_1, a_2), (a_3, a_4), (\lambda)\}$	1 296 14 025	6
ICR	$\{(\kappa, \bar{\kappa}, \tau, \bar{\tau}), (\lambda)\}$	96	61 870	$\{(a_2, a_3), (a_1, a_3), (\lambda)\}$ $\{(\bar{\kappa}, \tau), (\kappa, \bar{\tau}), (\lambda)\}$ $\{(\kappa, \bar{\tau}), (\tau, \bar{\kappa}), (\lambda)\}$	14 025 1 296 1 296	4
DHR	$\{(e_0, \dots, t_3)_h, (\lambda, \mu)\}$	165 240	–	$\{(e_0, \dots, t_3)_h, (\lambda), (\mu)\}$	194 400	$\frac{11}{17}$
QBR	$\{(e_0, \dots, t_2)_h, (\lambda, \mu)\}$	41 160	–	$\{(e_0, \dots, t_2)_h, (\lambda), (\mu)\}$	82 320	$\frac{7}{6}$

2.1 Results

The results are based on the example illustrated in Fig. 1. The system of n partial derivatives L_j ($j = 1, \dots, n$) of L results in all cases in a non-homogenous system of equations. The number n of unknown variables in this polynomial system is 5 for $\alpha \in S(2)$ and 6 for $\alpha \in SE(2)$. The total number of all possible groupings of the n variables is given by the so-called *Bell number*³ $B(n)$ with $B(5) = 52$ and $B(6) = 203$. For every representation all the possible groupings are tested by using default settings in Bertini 1.6v with a multi-homogeneous homotopy continuation method. We used Linux OS (Ubuntu 18.04) with a 1.80GHz Intel i5-6260U CPU. Comparison of Bézout numbers and degree of the Lagrange function (DOL) for all the presented representations are summarized in the Tables 1 and 2, where B_{min} and B_{max} indicates the Bézout number for best and worst groupings of unknown variables. We are also interested in average total tracking time T_{avg} in Milliseconds for B_{min} . We took T_{avg} because there will be variations in total tracking time for each run, depending upon the random seed chosen by Bertini.

To verify the solutions obtained by Bertini, we solved the polynomial system also in Maple 2018 using Gröbner basis method. In all cases the Maple solutions matched with those received from Bertini. The total number of solutions for all three representations are summarized in Table 3. For $\alpha \in SE(2)$ we get for PERR double the solutions of PBR and ICR as $\pm(a_1, a_2)$ describe the same rotation. For $\alpha \in S(2)$ we obtain for PERR 86 solutions, where 76 correspond to the 19 solutions of PBR and ICR as $\pm(a_1, a_2)$ and $\pm(-a_2i, a_1i)$ result in the same rotation matrix. The remaining 10 solutions (given in App. A) lie on the quadric $a_1^2 + a_2^2 = 0$ rendering this matrix singular.

Table 3 Total number of solutions (counted including multiplicity) for studied representations

Motion group	PBR and ICR	PERR	BGR and DCKR (Bertini)	BGR and DCKR (Maple)
SE(2)	32	64	162	32 & 1-dim set & 2-dim set
S(2)	19	86		

³ In case if $n > 6$ the Bell number $B(n)$ increases very quickly (see [2, p. 72, Table 5.1]).

3 Homogeneous Representations

In this section, we present two homogeneous algebraic representations for each of the motion groups SE(2) and S(2), respectively. Two of them are based on Study's kinematic mapping (e.g. [5, p. 86]), where each element of SE(3) is represented by a point $(e_0 : e_1 : e_2 : e_3 : t_0 : t_1 : t_2 : t_3)$ in the projective 7-dimensional space P^7 located on the so-called Study quadric given by

$$e_0 t_0 + e_1 t_1 + e_2 t_2 + e_3 t_3 = 0 \quad (8)$$

sliced along the 3-dimensional generator space $e_0 = e_1 = e_2 = e_3 = 0$.

Blaschke-Grünwald Representation (BGR): This representation is obtained by restricting Study's parametrization to the planar case i.e. $e_1 = e_2 = t_0 = t_3 = 0$. According to [5, p. 91] the transformation $\alpha : \mathbb{R}^2 \rightarrow \mathbb{R}^2$ can be written as:

$$\alpha : \mathbf{P}_i \mapsto \mathbf{P}_i^\alpha := \frac{1}{\Delta} \left[\begin{pmatrix} e_0^2 - e_3^2 & -2e_0 e_3 \\ 2e_0 e_3 & e_0^2 - e_3^2 \end{pmatrix} \mathbf{P}_i + \mathbf{t} \right] \quad (9)$$

with $\mathbf{t} := [-2(e_0 t_1 - e_3 t_2), -2(e_0 t_2 + e_3 t_1)]^T$, $\Delta := e_0^2 + e_3^2$ and $e_0, e_3, t_1, t_2 \in \mathbb{R}$. The computation of e_3 is based on the Lagrange function L given in Eq. (4).

Davidson-Hunt Representation (DHR): Based on the analogy of the Study parameters to homogenous screw coordinates (for details see e.g. [8, Section 1.1]) Davidson and Hunt [4, p. 409] suggested to interpret the points in the ambient space P^7 of the Study quadric as spatial similarity transformations. Following this idea and restricting it to S(2) we end up with the following representation of $\alpha : \mathbb{R}^2 \rightarrow \mathbb{R}^2$:

$$\alpha : \mathbf{P}_i \mapsto \mathbf{P}_i^\alpha := \frac{1}{\Delta^2} \left[(\Delta + e_0 t_0 + e_3 t_3) \begin{pmatrix} e_0^2 - e_3^2 & -2e_0 e_3 \\ 2e_0 e_3 & e_0^2 - e_3^2 \end{pmatrix} \mathbf{P}_i + \Delta \mathbf{t} \right] \quad (10)$$

with $e_0, e_3, t_0, t_1, t_2, t_3 \in \mathbb{R}$. The computation of s_3 is based on the Lagrange function (5) with the constraint $M := e_0 t_3 - e_3 t_0$.

Quaternion Based Representation (QBR): In [7, Section 2] a quaternionic formulation of S(4) and S(3) is given, which can also be restricted to S(2). Within this approach the transformation $\alpha : \mathbb{R}^2 \rightarrow \mathbb{R}^2$ reads as:

$$\alpha : \mathbf{P}_i \mapsto \mathbf{P}_i^\alpha := \frac{1}{\Delta} \left[\begin{pmatrix} e_0 f_0 - e_3 f_3 & -e_0 f_3 - e_3 f_0 \\ e_0 f_3 + e_3 f_0 & e_0 f_0 - e_3 f_3 \end{pmatrix} \mathbf{P}_i + \mathbf{t} \right] \quad (11)$$

with $e_0, e_3, f_0, f_3, t_1, t_2 \in \mathbb{R}$. The computation of s_3 is based on the Lagrange function (5) where the constraint M is given by $M := e_0 f_3 - e_3 f_0$.

Dual Cayley-Klein Representation (DCKR): By using the dual Cayley-Klein parameters of SE(2), which are introduced in [9], the isotropic point coordinates (z_i, \bar{z}_i) are transformed by $\alpha : \mathbb{C}^2 \rightarrow \mathbb{C}^2$ as follows:

$$\alpha : (z_i, \bar{z}_i) \mapsto (z_i^\alpha, \bar{z}_i^\alpha) := \frac{1}{\theta \bar{\theta}} (\theta(\theta z_i + 2\sigma), \bar{\theta}(\bar{\theta} \bar{z}_i + 2\bar{\sigma})) \quad (12)$$

with $\theta, \sigma, \tilde{\theta}, \tilde{\sigma} \in \mathbb{C}$. The homogenous 4-tuple $(\theta : \sigma : \tilde{\theta} : \tilde{\sigma})$ corresponds to a real displacement α if and only if there exists a value $c \in \mathbb{C} \setminus \{0\}$ such that $\overline{\theta}c = \tilde{\theta}c$ and $\overline{\sigma}c = \tilde{\sigma}c$ hold, which is equivalent to the condition $\tilde{\theta}\overline{\sigma} = \tilde{\sigma}\overline{\theta}$. The computation of e_3 is based on the Lagrange function L given in Eq. (4).

Remark 1. Note that according to [9], BGR and DCKR are linked by the relation: $e_0 = (\theta + \tilde{\theta})/2$, $e_3 = -i(\theta - \tilde{\theta})/2$, $t_1 = (\sigma + \tilde{\sigma})/2$ and $t_2 = -i(\sigma - \tilde{\sigma})/2$. \diamond

In summary, $\alpha \in \text{SE}(2)$ is given by homogenous 4-tuples $(e_0 : e_3 : t_1 : t_2)$ in BGR and $(\theta : \sigma : \tilde{\theta} : \tilde{\sigma})$ in DCKR. In contrast, $\alpha \in \text{S}(2)$ is determined by homogenous 6-tuple $(e_0 : e_3 : t_0 : t_1 : t_2 : t_3)$ in DHR and $(e_0 : e_3 : f_0 : f_3 : t_1 : t_2)$ in QBR.

3.1 Results

The following results are again based on the example illustrated in Fig. 1. In all cases the Lagrange function is rational⁴ where the polynomials in the numerator and denominator are homogenous and of the same degree with respect to the motion parameters m_1, \dots, m_k , where $k = 4$ holds for BGR and DCKR and $k = 6$ holds for DHR and QBR. Therefore the system of n partial derivatives L_j ($j = 1, \dots, n$) of L results in a homogenous system of equations with respect to m_1, \dots, m_k . Due to the homogeneity this polynomial system is overdetermined but it can easily be checked that the relation $\sum_{j=1}^k m_j \frac{\partial L}{\partial m_j} = 0$ holds. Bertini cannot handle overdetermined systems⁵ without the following user interaction: One has to square up the system [2, p. 14] by replacing the k equations $\frac{\partial L}{\partial m_j} = 0$ for $j = 1, \dots, k$ by $k - 1$ linear combinations of the form $\sum_{j=1}^k \square \frac{\partial L}{\partial m_j}$ where each \square indicates a randomly chosen complex number. The resulting system can then be passed on to Bertini by using the command `hom_variable_group` for grouping the homogenous variables m_1, \dots, m_k into one group, which is indicated in Tables 1 and 2 by the notation $(m_1, \dots, m_k)_h$. Therefore there is only one possible grouping for BGR and DCKR and two possible groupings for DHR and QBR. For both of these groupings the resulting Bézout numbers are too large (cf. Table 2) to expect reasonable computation times thus we abstained from tracking the paths.

All additional 130 solutions received by Bertini based on BGR and DCKR (cf. Table 3) fulfill $\Delta = 0$ resp. $\theta\tilde{\theta} = 0$ implying a division by zero in Eq. (9) resp. (12). But it turns out that 128 of these solutions either result from squaring up the system [2, p. 15] (cf. Apps. B and C) or belong to the 2-dimensional solution set⁶ $e_0 = e_3 = 0$ resp. $\theta = \tilde{\theta} = 0$. There also exists a 1-dimensional solution set⁶ (cf. Apps. B and C), which corresponds to two conics on the hyperquadric $\Delta = 0$ resp. $\theta\tilde{\theta} = 0$. The remaining two solutions represent a point on each of these two curves.

⁴ The degrees of the polynomials in the numerator and denominator with respect to all n unknowns are given as fraction (deg numerator)/(deg denominator) in the column DOL of Tables 1 and 2.

⁵ In contrast to the software package HomotopyContinuation.jl [3].

⁶ Positive-dimensional solution sets cannot be detected by Bertini using default settings.

4 Conclusions

It can be observed (cf. Table 1) that the B_{min} value obtained for ICR is the best one of all SE(2) representations as suggested in [2, p. 96]. For S(2) the lowest number of tracked paths is obtained by ICR and PBR (cf. Table 2). Surprisingly the PBR has in both motion groups by far the best computational performance with respect to T_{avg} . It can also be seen by B_{max} that the grouping has huge effects on the number of tracked paths and therefore on the computation time. Moreover, due to the large Bézout numbers of DHR and QBR the question arises whether a computationally more efficient homogenous representation of S(2) exists.

All in all, this study suggests the usage of PBR for the future research on the spatial case (i.e. hexapods and linear pentapods) due to the good B_{min} values and the best results for T_{avg} .

Acknowledgements This research is supported by the Grant No.P 30855-N32 of the Austrian Science Fund FWF. The first author would like to thank Arvin Rasoulzadeh for his valuable suggestions and technical discussions.

References

1. Bates, D.J., Hauenstein, J.D., Sommese, A.J., Wampler, C.W.: Bertini: Software for numerical algebraic geometry. Available at bertini.nd.edu with permanent doi: [dx.doi.org/10.7274/R0H41PB5](https://doi.org/10.7274/R0H41PB5)
2. Bates, D.J., Sommese, A.J., Hauenstein, J.D., Wampler, C.W.: Numerically solving polynomial systems with Bertini. SIAM (2013)
3. Breiding, P., Timme, S.: Homotopycontinuation.jl: A package for homotopy continuation in julia. In: J.H. Davenport, M. Kauers, G. Labahn, J. Urban (eds.) Mathematical Software – ICMS 2018, pp. 458–465. Springer (2018)
4. Davidson, J.K., Hunt, K.H.: Robots and Screw Theory: Applications of kinematics and statics to robotics. Oxford University Press (2004)
5. Husty, M.L., Schröcker, H.P.: Kinematics and algebraic geometry. In: J.M. McCarthy (ed.) 21st Century Kinematics, pp. 85–123. Springer (2013)
6. Li, T., Bai, F.: Minimizing multi-homogeneous Bézout numbers by a local search method. Mathematics of Computation **70**(234), 767–787 (2001)
7. Nawratil, G.: Quaternionic approach to equiform kinematics and line-elements of Euclidean 4-space and 3-space. Computer Aided Geometric Design **47**, 150–162 (2016)
8. Nawratil, G.: Kinematic interpretation of the Study quadrics ambient space. In: J. Lenarcic, V. Parenti-Castelli (eds.) Advances in Robot Kinematics, pp. 3–11. Springer (2018)
9. Nawratil, G.: Parallel manipulators in terms of dual Cayley-Klein parameters. In: S. Zeghloul, L. Romdhane, M. Laribi (eds.) Computational Kinematics, pp. 265–273. Springer (2018)
10. Nawratil, G.: Singularity distance for parallel manipulators of Stewart Gough type. In: T. Uhl (ed.) Advances in Mechanism and Machine Science, pp. 259–268. Springer (2019)
11. Wampler, C.W.: Bezout number calculations for multi-homogeneous polynomial systems. Applied Mathematics and Computation **51**(2-3), 143–157 (1992)
12. Wampler, C.W., Sommese, A.J.: Applying numerical algebraic geometry to kinematics. In: J.M. McCarthy (ed.) 21st Century Kinematics, pp. 125–159. Springer (2013)

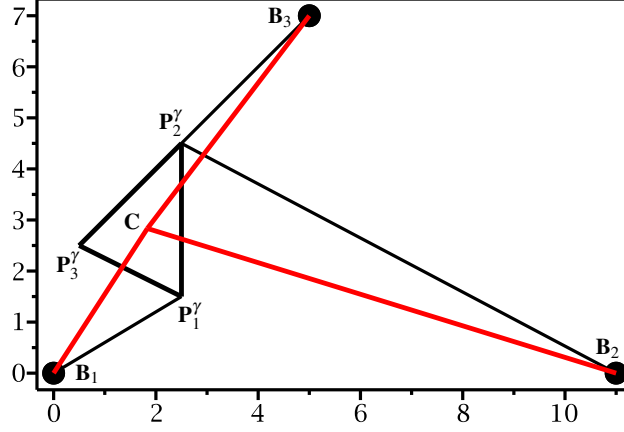


Fig. 2 Illustration of the double solution: The platform degenerates to the centroid C (yielding the red singular configuration) of the moving platform in the given pose (displayed in black).

Appendix

A. Additional ten solutions of PERR under equiform motions

In the following we give the explicit expressions of the 10 solutions mentioned in Sec. 2.1 lying on the quadric $a_1^2 + a_2^2 = 0$.

Solutions 1 and 2: The real solution $a_1 = 0, a_2 = 0, a_3 = \frac{11}{6}, a_4 = \frac{17}{6}$ is of multiplicity 2. In this case the platform degenerates to the centroid C of the moving platform in the given pose (cf. Fig. 2).

Solutions 3–6: The third solution is given by:

$$a_1 = \frac{\sqrt{w_0} \sqrt{(w_1 - w_2 i) + \sqrt{\frac{(w_3 + w_4 i)}{w_5}}}}{w_6}, \quad a_3 = u_0 + u_1 i - \frac{b_1 \sqrt{w_3 + w_4 i}}{k_1} - \frac{n_1 i \sqrt{-w_3 - w_4 i}}{k_2},$$

$$a_2 = \frac{-i \sqrt{(r_0 - r_1 i) + 2 \sqrt{\frac{(w_3 + w_4 i)}{w_5}}}}{w_6}, \quad a_4 = q_0 - q_1 i - \frac{b_2 \sqrt{w_3 + w_4 i}}{k_3} + \frac{n_2 i \sqrt{-w_3 - w_4 i}}{k_4}$$

with $w_0 = 2, w_1 = 31779207, w_2 = 30431636, w_3 = 120733747144604, w_4 = 831183587338, w_5 = 21040857161, w_6 = 3796, r_0 = 63558414, r_1 = 60863272, u_0 = -\frac{17446123}{3602404}, u_1 = \frac{46887293}{1801202}, q_0 = -\frac{21374427}{3602404}, q_1 = \frac{1811805}{900601}, b_1 = 18854507559, b_2 = 52996212054, n_1 = 52996212054117$ and $n_2 = 14299077184932$. The other

three solutions for (a_1, a_2, a_3, a_4) equal $(-a_1, -a_2, a_3, a_4)$ and $(\pm a_2 i, \mp a_1 i, a_3, a_4)$, respectively.

Solutions 7–10: The seventh solution is given by:

$$a_1 = \frac{\sqrt{w_0} \sqrt{(w_1 + w_2 i) + \sqrt{\frac{(-w_3 + w_4 i)}{w_5}}}}{w_6}, \quad a_3 = u_0 - u_1 i - \frac{b_1 \sqrt{-w_3 + w_4 i}}{g_1} - \frac{n_1 i \sqrt{-w_3 + w_4 i}}{g_2},$$

$$a_2 = \frac{i \sqrt{(r_0 + r_1 i) + 2 \sqrt{\frac{(-w_3 + w_4 i)}{w_5}}}}{w_6}, \quad a_4 = q_0 + q_1 i - \frac{b_2 \sqrt{-w_3 + w_4 i}}{g_3} + \frac{n_2 i \sqrt{-w_3 + w_4 i}}{g_4}$$

with $g_1 = 772036659995716$, $g_2 = 38601832999$, $g_3 = 77203665999$ and $g_4 = 19300916499$. The other three solutions for (a_1, a_2, a_3, a_4) equal $(-a_1, -a_2, a_3, a_4)$ and $(\pm a_2 i, \mp a_1 i, a_3, a_4)$, respectively.

B. Computational details of BGR

Maple computations: It can be verified using Gröbner basis method that the polynomial system does not only have 32 isolated solutions and the 2-dimensional solution set $e_0 = e_3 = 0$ but also a 1-dimensional solution set given by:

$$e_0 = 1, \quad e_3 = \pm i \quad \text{and} \quad (13)$$

$$3752e_3 t_1 - 13723e_3 t_2 + 1865t_1^2 + 1865t_2^2 + 8629t_1 + 2144t_2 = 0.$$

Therefore it corresponds to two conic sections on the quadric $e_0^2 + e_3^2 = 0$.

Bertini computations: We squared up the system of equations as described in Sec. 3.1 by using the numerators of the following three linear combinations:

$$(1 - 7i) \frac{\partial L}{\partial e_0} + (2 - 3i) \frac{\partial L}{\partial e_3} + (3 + 5i) \frac{\partial L}{\partial t_1} + (4 - 6i) \frac{\partial L}{\partial t_2},$$

$$(4 + 2i) \frac{\partial L}{\partial e_0} + (3 - 3i) \frac{\partial L}{\partial e_3} + (3 - 2i) \frac{\partial L}{\partial t_1} + (3 + 5i) \frac{\partial L}{\partial t_2},$$

$$(2 + 3i) \frac{\partial L}{\partial e_0} + (3 - 5i) \frac{\partial L}{\partial e_3} + (2 - 2i) \frac{\partial L}{\partial t_1} + (3 - 3i) \frac{\partial L}{\partial t_2}.$$

Based on this input the 130 additional solutions obtained by Bertini split up in the following way: We get one solution on each of the conic sections given in Eq. (13), 39 solutions belong to the 2-dimensional solution set $e_0 = e_3 = 0$ and 89 solutions result from squaring up the system (they do not fulfill the initial set of equations).

Remark 2. All 130 additional solutions depend on the random seed chosen by Bertini; even the number of solutions belonging to the 2-dimensional set is not constant. But it turns out in all our examples that exactly two solutions are located on the 1-dimensional set (one on each conic section). \diamond

C. Computational details of DCKR

Maple computations: The polynomial system has 32 isolated solutions, the 2-dimensional solution set $\theta = \tilde{\theta} = 0$ and a 1-dimensional solution set, which corresponds to the following two conic sections:

$$\begin{aligned} \theta = 0, \quad \tilde{\theta} = 1, \quad 1865\tilde{\sigma}\sigma + 2547\tilde{\sigma} + 804i\tilde{\sigma} - 11176\sigma + 2948i\sigma &= 0, \\ \theta = 1, \quad \tilde{\theta} = 0, \quad 1865\tilde{\sigma}\sigma + 2547\sigma - 804i\sigma - 11176\tilde{\sigma} - 2948i\tilde{\sigma} &= 0. \end{aligned} \quad (14)$$

Bertini computations: We squared up the system of equations as described in Sec. 3.1 by using the numerators of the following three linear combinations:

$$\begin{aligned} (3-i)\frac{\partial L}{\partial \theta} + (3-4i)\frac{\partial L}{\partial \tilde{\theta}} + (2-3i)\frac{\partial L}{\partial \sigma} + (5-4i)\frac{\partial L}{\partial \tilde{\sigma}}, \\ (1-2i)\frac{\partial L}{\partial \theta} + (3-5i)\frac{\partial L}{\partial \tilde{\theta}} + (2-3i)\frac{\partial L}{\partial \sigma} + (5-5i)\frac{\partial L}{\partial \tilde{\sigma}}, \\ (7-i)\frac{\partial L}{\partial \theta} + (3-2i)\frac{\partial L}{\partial \tilde{\theta}} + (1-2i)\frac{\partial L}{\partial \sigma} + (5-2i)\frac{\partial L}{\partial \tilde{\sigma}}. \end{aligned}$$

Based on this input the 130 additional solutions obtained by Bertini split up in the following way: We get one solution on each of the conic sections given in Eq. (14), 41 solutions belong to the 2-dimensional solution set $\theta = \tilde{\theta} = 0$ and 87 solutions result from squaring up the system (they do not fulfill the initial set of equations).

Finally it should be mentioned that Remark 2 is also valid for this case.